Northern Hemisphere Five-Year Average (2000-2004) Spectral Albedos of Surfaces in the Presence of Snow: Statistics Computed from Terra MODIS Land Products

ERIC G. MOODY,* MICHAEL D. KING,† CRYSTAL B. SCHAAF,‡
DOROTHY K. HALL,§ AND STEVEN PLATNICK†

**RS Information Systems, Inc., Lanham, Maryland*
†*Earth Sciences Division, NASA Goddard Space Flight Center, Greenbelt, Maryland*
‡*Center for Remote Sensing, Department of Geography, Boston University, Boston, Massachusetts*
§*Cryospheric Sciences Branch, NASA Goddard Space Flight Center, Greenbelt, Maryland*

Remote Sensing of Environment

(Manuscript submitted 21 August 2006, revision submitted 21 November 2006, final submission 13 December 2006)

Corresponding author address: Eric G. Moody, RS Information Systems, Inc., Lanham, MD 20706 USA.

E-mail: moody@climate.gsfc.nasa.gov.

Abstract

In this paper, we present five-year (2000-2004) climatological statistics of Northern Hemisphere spectral white-sky albedo for the 16 International Geosphere-Biosphere Program (IGBP) ecosystem classes when accompanied by the presence of snow on the ground. These statistics are obtained using validated, high quality Moderate Resolution Imaging Spectroradiometer (MODIS) land surface albedo (MOD43B3) data flagged as snow in the associated Quality Assurance (QA) fields. Near Real-Time Ice and Snow Extent (NISE) data are used as an additional discriminator of snow extent. Statistics are provided for the first seven MODIS bands, ranging from 0.47 to 2.1 μm, and for three broadbands, 0.3-0.7, 0.3-5.0 and 0.7-5.0 μm.

The statistics demonstrate that each ecosystem classification has a discernible spectral albedo signature when accompanied by snow on the ground. This indicates that winter canopy and underlying surface radiative properties are impacted by the presence of snow overlying these surfaces. For example, the 0.47 μm albedo of winter snow-free evergreen needleleaf forests increases from 0.03 to 0.36 in the presence of snow, compared to an increase of 0.04 to 0.76 for croplands. In general, the albedo of snow-covered ecosystems with some winter canopy have lower albedos than ecosystems with little to no winter canopy; for example the 0.47 μm albedo of snow-covered mixed forests is 0.39 compared to 0.87 for barren/deserts and 0.95 for permanent snow.

These statistics can be used within land surface models in a stand-alone mode, to prescribe albedo values in atmospheric General Circulation Models (GCMs), or be incorporated into research and operational projects. They are intended to provide researchers with representative spectral albedo values of IGBP ecosystems in the presence of snow that are derived from validated satellite data.

1. Introduction

The ratio of reflected to incident radiation, or albedo, of a surface in the presence of snow can be influenced by several characteristics. During periods that coincide with snow coverage, the vegetation is either at or near the full dormant (winter) state; however, the remnants of the vegetative canopy can protrude from the surface. As such, differences in dormant snow-free surface conditions for the various land surface classifications result in distinct ecosystem spectral signatures (see for example Moody et al., 2005). However, the presence of snow, the location of the snow (on or below winter canopies), and the condition of the snow (i.e. snow state, morphology, age, depth, type, and contamination, among others) can dramatically alter these spectral signatures.

Proper representation of the impact of snow on the snow-free surface albedo thereby becomes critical for Earth system remote sensing, energy budgeting, and modeling projects that depend on surface radiative properties for accurate observations and calculations of Earth and atmosphere properties. As such, the goal of the present study is to employ validated remote sensing data to provide researchers with representative albedo values for the various ecosystems while they are in the presence of snow. To accomplish this, we utilize validated observations of land surface classification (MOD12Q1, Friedl et al., 2002) and land surface albedo (MOD43B3, 16-day product, Schaaf et al., 2002) that are readily available from the Moderate Resolution Imaging Spectroradiometer (MODIS) onboard NASA's Terra (King and Herring, 2000) satellite.

The analysis is not straightforward, however, as some of these snow and surface properties can change quite dramatically over a 16-day period of MODIS albedo observations. Additionally, MOD43B3 albedo observations are by nature a temporal average of changing conditions, except in very limited regions of continuity. Further complicating matters, correlating albedo observations with these snow and surface properties is hampered by the limited availability of high-resolution temporal and spatial data. This includes a limited number of highest quality MOD43B3 snow albedo observations over both a 16-day period and even over the course of a full year.

Instead, this work provides albedo values for surfaces in the presence of "average" snow conditions by computing ecosystem-dependant multi-year northern hemisphere statistics (Jin et al., 2002). Such statistics are an amalgamation of the differing snow conditions that occur during the course of the snow season for each ecosystem type. This is accomplished by using all of the highest-quality MOD43B3 observations (discerned to be snow) in the Northern Hemisphere over nearly five years (March 2000-December 2004).

The resulting statistics of surface albedo in the presence of snow provide researchers with reasonable and representative spectral albedo values at seven discrete wavelengths between 0.47 and 2.1 μm, and three broadbands, 0.3-0.7, 0.3-5.0, and 0.7-5.0 μm that are derived from validated satellite data. The statistics may be used as a stand-alone lookup table, or incorporated into remote sensing retrievals by matching conditions to a lookup table of these average snow conditions. They may also be an excellent source for model validation.

This paper explores the techniques and datasets used to compute the statistics of the surface albedo in the presence of snow and proceeds by providing background on albedo applications and data sources (section 2), an overview of the methodology, including a description of the data used and conditioning and statistical calculations (section 3), and finally a discussion of the resulting data (section 4), and potential applications (section 5).

2. Background

The albedo of a surface in the presence of snow is a key parameter for remote sensing of atmospheric cloud properties and plays a central role in global energy budget and climate forcing issues (Dickinson, 1992; Viterbo and Betts, 1999; Roesch et al., 2002; Platnick et al., 2003; King et al., 2004). Various climatic and ecosystem models, at a variety of scales, use snow-free albedo maps with superimposed snow properties (extent, type, albedo, etc.) (Dickinson et al., 1986; 1988; Barnett et al., 1989; Verseghy, 1991; Cess et al., 1991; Bonan, 1996; Yang et al., 1999; Molotch and Bales, 2006; Molotch et al., 2004). Remote sensing projects depend on the knowledge of surface radiative properties for accurate observations of Earth and atmosphere properties.

Aircraft and satellite observations of snow-covered land surfaces have been undertaken for many years; various techniques have been used to derive albedo over a variety of land-cover types (see for example, McFadden and Ragotzkie, 1967; Robinson and Kukla, 1985; Dozier, 1989). There have also been extensive efforts to model the effects of various influencing factors (snow state, contamination, etc.) on the albedo of snow-covered surfaces (Wiscombe and Warren, 1980; Warren and Wiscombe, 1980; Warren, 1982; Dozier et al., 1981; Grenfell and Warren, 1994; Davis et al., 1997; Nolin and Dozier, 2000; Painter and Dozier, 2004).

There have also been some remote sensing, ground, and laboratory validation projects that have provided observations under a variety of conditions (Stroeve et al., 2005, Salomonson and Marlatt, 1968; O'Brien and Munis, 1975; Brest and Goward, 1987; Hall et al., 1993; Betts and Ball, 1997; Klein and Stroeve, 2002; Liang et al., 2002, 2005; Greuell and Oerlemans, 2005; Arnold et al., 2002; Grenfell and Perovich, 2004). These studies have shown that the albedo of surfaces in the presence of snow can vary dramatically, and therefore must be taken into account in radiative transfer calculations.

While the MOD43B3 product is currently the only validated source of global high-resolution snow-covered surface albedo data, the MOD10 Terra MODIS product suite (Hall et al., 2006 & in press) can be used as an additional source for daily snow-coverage and snow albedo products. The MOD10 snow albedo data are an initial effort and currently only designated as "provisionally validated," but the snow-covered area data product is very mature and is validated to stage 2. In the future, it would be beneficial to use the validated MOD10 snow-covered area data to crosscheck the MOD43B3 data for the presence of snow as the MOD10 product's spatial resolution is 500 meters, and includes sub-pixel snow-cover information.

3. Methodology and Datasets

As an overview, nearly five years (March 2000- December 2004) of the highest quality Northern Hemisphere MOD43B3 albedo observations, discerned to be snow (through internal MOD43B3 flags and Near Real-Time Ice and Snow Extent (NISE) data), are aggregated by the International Geosphere-Biosphere Program (IGBP) land surface classifications. The mean, standard deviation, and the coefficient of variation (standard deviation normalized by the mean) are then computed from this aggregated data. To provide additional comparisons, similar statistics are computed from highest quality pixels that are deemed to be free of snow.

Before computing the statistics, the three datasets used, MODIS albedo and land cover classification, and NISE, are conditioned and reprojected onto a common grid with one-minute resolution in geographical coordinates. The daily

NISE data are also aggregated to match the MODIS albedo 16-day period. The ensuing subsections detail these procedures.

3.1 MODIS albedo dataset and conditioning

The launch of the Moderate Resolution Imaging Spectroradiometer (MODIS) onboard NASA's *Terra* spacecraft in December 1999 (King and Herring, 2000) ushered in a wealth of new products with unprecedented spectral, spatial, and temporal characteristics. Of particular interest to this study is the operational diffuse bihemispherical (white-sky) and direct beam directional hemispherical (black-sky) land surface albedo dataset, known as MOD43B3 (Schaaf et al., 2002). In this study, only the white-sky albedo is considered due to it being independent of angular effects; the black-sky albedo is computed at an angle of local solar noon. This product is a validated 16-day aggregate global dataset at 1 km spatial resolution for the first seven MODIS bands, 0.47 through 2.1 μm, and for three broadbands, 0.3-0.7, 0.3-5.0, and 0.7-5.0 μm (Schaaf et al., 2002).

Recent validation efforts have shown that the MODIS "high quality" albedo retrievals accurately represent the general snow conditions over the pure-snow conditions of the Greenland Ice Sheet (Stroeve et al., 2005). In the context of the MODIS albedo product, the term "high quality" has a very specific meaning; it refers to retrievals that had seven or more non-obscured observations with sufficient angular sampling over the product's 16-day period to provide a well-defined Bidirectional Reflection Distribution Function (BRDF).

It is interesting to note that, to a first order approximation, uniform snow fields have forward-scattering BRDF properties, whereas wind sculpted and vegetated surfaces have back-scattering BRDF properties. In reality, at 1 km resolution almost every pixel will be impacted by melting pools, terrain variation, and extruding vegetation or significant canopies. The validation efforts (Stroeve et al., 2005) have shown that the MOD43B3 algorithm, which includes shadowing models, captures the proper geometric-optical effects over both flat, uniform, pure snow surfaces and non-uniform or winter canopy laden surfaces.

MOD43B3 data are stored using a sinusoidal (SIN) projection through a series of approximately 400 tiles (10° x 10° per tile). To facilitate analysis, the raw data are mosaiced onto a common grid with one-minute resolution in geographical coordinates, which is ~2 km in spatial resolution at the equator. This procedure is a sampling process for which the grid is defined and the data from the nearest geolocated pixel in the MODIS tile are geospatially translocated onto the common one-minute resolution, in geographical coordinates, grid.

MOD43B3 pixels that were covered with snow for more than half of the cloud-free observations over the 16-day period are flagged as such in the MOD43B3 Quality Assurance (QA), and only these snowy pixels are considered for inclusion in the statistics. To ensure that the resulting statistics provide the most accurate values possible, the pixels are further conditioned by applying the MODIS albedo product QA to remove pixels of lower quality. As detailed in the MODIS BRDF/albedo product (MOD43B) user's guide and Schaaf et al. (2002), only pixels with seven or more diverse angular observations over the 16-day period were included in the statistics. These pixels had sufficiently well sampled and high quality observations to have confidence in the retrieved albedo value (i.e., a well defined BRDF).

3.2 MODIS ecosystem classification dataset and conditioning

The interplay between the vegetative canopy, the underlying surface properties associated with land cover classification, and the snow can influence the radiative properties of the surface. For example, tree canopies can obscure surface snow and lower the reflectivity of the scene (e.g., Betts and Ball, 1997; Pomeroy and Dion, 1996; McFadden and Ragotzkie, 1967; Bounoua et al., 2000).

To compile the ecosystem-dependant statistics, the static MOD12Q1 ecosystem classification product, which represents the dominant land cover class for each pixel (Friedl et al., 2002), is also reprojected onto a common grid with one-minute resolution in geographical coordinates. At present, no QA is applied to the reprojected IGBP map, and only the predominant ecosystem classification is used for each pixel. In reality, most pixels will contain various classifications that may contribute to the variability in this study's ecosystem-dependant statistics.

3.3 NISE snow classification dataset and conditioning

In addition, the daily 15-minute x 15-minute horizontal resolution Near Real-Time Ice and Snow Extent (NISE) product that is derived from satellite-borne microwave radiometers (Armstrong and Brodzik, 2002) is used to further discriminate pixels identified as snow by the MOD43B3 QA flags. This product is not validated, however, and being a microwave product, it consistently does not detect thin snow; on the other hand, it is unlikely that thin snow would persist over a MOD43B3 datasets' 16-day period. Despite these negative aspects, this product can often provide valuable information.

In practice, the 15-minute NISE daily snow extent product was first projected onto the same common grid with one-minute resolution in geographical coordinates. The 16-day cycle of the MOD43B3 data is matched and the number of days during this period in which NISE flags a pixel as snow is computed. Of the high quality pixels labeled as snow by MOD43B3, only the pixels that are flagged as snow by NISE for over 90% of the days during the 16-day period are included in these statistics. Although the NISE product's spatial resolution is coarser than the MOD43B3 product, the conservative temporal criterion possible with the NISE data ensures that the albedos being utilized in this paper are more heavily and consistently snow-covered, and less likely to include albedos retrieved in the presence of some datable thin or patchy snow in the pixel.

4. Results and Discussion

The mean, standard deviation, and coefficient of variation for surfaces in the presence of snow were computed using nearly five years of MODIS data. The number of pixels used (not shown) to compute these statistics ranged from a high of nearly 80 million pixels for permanent snow, to a low of only 6,000 pixels for the evergreen broadleaf forest. Nine ecosystems had over a million pixels; another four had over 100,000 pixels, while another two had over 10,000 pixels. As such, these quantities should provide representative statistics.

Northern Hemisphere five-year mean spectral white-sky albedos for various ecosystems in the presence of snow are presented in Table 1 and Fig. 1, with accompanying standard deviations in Table 2. These illustrations demonstrate that each of the 16 IGBP ecosystem classes has a discernible spectral signature, with a maximum departure of 60% at a wavelength of 0.47 μm. Surfaces that are devoid, or nearly so, of vegetation during the winter have the highest albedo (such as barren or desert, permanent snow, and cropland). Please note that in Fig. 1 albedo values of discrete MODIS spectral bands are connected with straight lines for the sake of presentation only; absorption features between MODIS bands (e.g., vicinity of 1.5 μm, Grenfell and Perovich, 2004) are not shown.

Ecosystems that have some vegetative canopy generally have a lower albedo. Canopied ecosystems exhibit a peak around 0.86 μm that suggests contribution by the snow on the canopy (leaf/needle or otherwise). Evergreen needleleaf forests have the lowest overall spectral albedo, undoubtedly due to the relatively lush winter canopy that obscures the ground-level snow. The deciduous broadleaf and deciduous needleleaf forests have nearly identical spectral signatures, as their winter canopies (of dense branches) are similar. These results are in accordance with modeling studies that show canopies that cover snow reduce the surface albedo during winter times (Bonan, 1997, Bounoua et al., 2000).

In comparison to similarly computed snow-free dormant mean spectral signatures, shown in Figs. 2 and 3, the presence of snow generally increases the albedo in the 0.47 μm through 0.86 μm channels, while generally decreasing the albedo in the near- and short-wave infrared channels (1.24 μm – 2.13μm). Interestingly, these trends generally hold when comparing the albedo of snow-covered surfaces to the full growth spectral signatures.

Figs. 2 and 3 also illustrate the temporal change in the spectral signature of various ecosystems' surfaces in the presence of snow; five-year monthly averages are computed in a manner similar to that described in Sec. 3, except the latitudes are limited between 70° and 40° N to match the regions of dominant snow coverage. When interpreting the plots, note that the vast majority (not shown) of each ecosystem's snow-covered pixels occur in the months of January through March. In general, the spectral signatures are smallest in November and December (due to more ephemeral or mixed snow), increase during January and February (as the snow base builds), peak in March, and then decline in April (as melt pools and ephemeral/mixed snow conditions dominate). As these statistics are generated from the angle-independent (diffuse) white-sky albedo product, these temporal results are independent of sun angle to the extent that the bidirectional reflectance models used to derive the diffuse albedo are correct.

The variability in the mean spectral signatures of the various ecosystems in the presence of snow can be explored with the standard deviations (Table 2) and the coefficients of variability (Fig. 4). An appreciable amount of variability can be expected as the statistics are computed using data that cover five years and an entire hemisphere. Contributing factors include snow-free surface conditions (i.e., inter-ecosystem regional differences in decay state) and snow conditions (i.e., type, melt, depth, etc). Indeed the standard deviation values in Table 2 bear this out.

Perhaps a more appropriate method for comparing variability between datasets, however, is to compare the coefficients of variation, Fig. 4, as this statistical measure is in essence a non-dimensional and normalized standard deviation. Overall, this figure reiterates that there is appreciable, but expected, variability in the five-year Northern Hemispheric statistics. Upon examination of the 0.47 μm through 0.86 μm range, one finds that the least variable ecosystems are the ones with limited to no winter canopy, while the most variable are those ecosystems with significant winter canopies. In particular, the most variable ecosystems in this range are the Evergreen and Mixed Forests, whose canopies can retain highly variable and sometimes substantial amounts of snow. In addition, snow within these canopies can suddenly fall or be blown off which in turn dramatically alters the albedo of the scene.

The variability in this range also arises from the degree of the ecosystems' surface homogeneity; sample size does not appear to play a factor as, for example, the mixed forest (largest variability) and the barren desert (second smallest variability) classifications have 2.3 million and 4.5 million sample pixels, respectively. The spatial distribution of sample pixels can also contribute to the variability as local decay states and winter canopies may differ. Note that the coefficients become more erratic as they approach the 2.13 μm range as the denominators become small (mean albedo values as low as 0.04).

5. Example Applications

The spectral signatures of surfaces accompanied by snow presented in section 4 can be incorporated into a wide variety of Earth system modeling and remote sensing or ground-based research projects. One such example of integration is to use these values in tandem with the snow-free spatially complete surface albedo maps (Moody et al., 2005 & 2007) to provide dynamically tailored surface albedo maps. For example, uncoupled land surface parameterization models (LSPs) can be initialized, for a particular discrete wavelength, with a 16-day spatially complete surface albedo map that is snow-free. Using the land cover classification and the snow extent maps one can then compute the snow albedo using statistics from the lookup table. This albedo value can either be used to drive the LSPs in resolving the surface energy balance or used as validation fields for model computed albedo.

Alternatively, once snow extent and the underlying ecosystem class are defined, snow cover albedo values can be directly overlaid onto the map using Table 1. Figure 5 provides an illustration of such a process for the 0.86 μm data from January 1-16, 2002, in which NISE snow extent and snow type define the snow properties, and the 2000-2004 snow albedo statistics provide the albedo values. This type of procedure is currently being used operationally in the MODIS cloud optical properties product (MOD06/MYD06) (Platnick et al., 2003, King et al., 2003) as well as in the retrievals of aerosol properties from ground-based Aerosol Robotic NETwork (AERONET) sunphotometer observations

(Holben et al., 1998; Dubovik et al., 2000).

Besides the tabular format provided in Tables 1 and 2, the data are available in an Hierarchical Data Format (HDF) data file. This data file also includes the number of pixels used to provide the statistical information. The data file is available for public download via an anonymous ftp site at ftp://modis-atmos.gsfc.nasa.gov.

6. Summary

In this paper, we present five-year Northern Hemisphere spectral albedo statistics (mean, standard deviation, and coefficient of variation) for the 16 IGBP ecosystem surfaces when accompanied by snow. These statistics are computed for each of the 10 MOD43B3 narrowband and broadband wavelengths. The analysis demonstrates that each ecosystem classification has a discernible spectral albedo signature when accompanied by snow on the ground. This indicates that winter canopy and underlying surface radiative properties are impacted by the presence of snow overlying these surfaces.

It is the intention of the authors to provide researchers with representative spectral albedo values of IGBP ecosystems in the presence of snow that are derived from validated satellite data. It is anticipated that these statistics will be incorporated within land surface models in a stand-alone mode, to prescribe albedo values in atmospheric General Circulation Models (GCMs), or be incorporated into research and operational projects.

Acknowledgments

The research reported in this article was supported by EOS MODIS support, the MODIS Science Team under NASA contract 621-30-H4, and to Goddard Space Flight Center (E.G. Moody, M.D. King, D.K. Hall, S. Platnick) and NASA contract NAS5-31369 to Boston University (CBS). The authors would like to express their appreciation to Dr. Lahouari Bounoua, Goddard Space Flight Center, for providing valuable insight into modeling community requirements and reviewing the methodologies used in this work, and to Dr. Reto Stockli, National Center for Atmospheric Research, for his expertise in crafting Figure 5.

References

Armstrong, R. L., & Brodzik, M. J. (2002), Hemispheric-scale comparison and evaluation of passive-microwave snow algorithms. *Annals of Glaciology*, *34*, 38–44.

Arnold, G. T., Tsay, S. C., King, M. D., Li, J. Y., & Soulen, P. F. (2002), Airborne spectral measurements of surface-atmosphere anisotropy for Arctic sea ice and tundra. *International Journal of Remote Sens*ing, *23*, 3763–3781.

Barnett, T. P., Dumenil, L., Schlese, U., Roeckner, E., & Latif, M. (1989), The effect of Eurasian snow cover on regional and global climate variations. *Journal of the Atmospheric Sciences*, *46*, 661–685.

Betts, A. K., & Ball, J. H. (1997), Albedo over the boreal forest. *Journal of Geophysical Research,* 102, 28901–28909.

Bonan, G. B. (1996), *A Land Surface Model (LSM version 1.0) for Ecological, Hydrological, and Atmospheric Studies: Technical Description and User's Guide*. NCAR Tech. Note NCAR/TN2417ISTR, National Center for Atmospheric Research, Boulder, CO, 150 pp.

Bonan, G. B. (1997), Effects of land use on the climate of the United States. *Journal of Climatic Change*, *37*, 449–486.

Bounoua, L., Collatz, G. J., Los, S. O., Sellers, P. J., Dazlich, D. A., Tucker, C. J. & Randall, D. (2000), Effects of land cover conversion on surface climate. *Journal of Climate*, *13*, 2277–2292.

Brest, C. L., & Goward, S. N. (1987), Deriving surface albedo measurements from narrow band satellite data. *International Journal of Remote Sensing*, *8*, 351–367.

Cess, R. D., & Coauthors (1991), Intercomparison of snow-feedback as produced by general circulation models. *Science*, *253*, 888–892.

Davis, R. E., Hardy, J. P., Ni, W., Woodcock, C., McKenzie, C. J., Jordan, R., & Li, X. (1997), Variation of snow ablation in the boreal forest: A sensitivity study on the effects of conifer canopy. *Journal of Geophysical Research, 102*(D24), 29389–29396.

Dickinson, R. E. (1988), The force-restore model for surface temperature and its generalizations. *Journal of Climate*, *1*, 1086–1097.

Dickinson, R. E. (1992), Land Surface. In *Climate System Modeling*, edited by K. E. Trenberth, Cambridge University Press, pp. 149–171.

Dickinson, R. E., Henderson-Sellers, A., Kennedy, P. J., & Wilson, M. F. (1986), *Community Climate Model*, NCAR Tech. Note NCAR/TN2275ISTR, National Center for Atmospheric Research, Boulder, CO, 69 pp.

Dozier, J. (1989), Spectral signature of alpine snow cover from the Landsat Thematic Mapper. *Remote Sensing of Environment*, *28,* 9–22.

Dozier, J., Schneider, S. R., & McGuiness, D. F. (1981), Effect of grain size and snowpack water equivalence on visible and near-infrared satellite observations of snow. *Water Resources Research*, *17*, 1213–1221.

Dubovik, O., Smirnov, A., Holben, B. N., King, M. D., Kaufman, Y. J., Eck, T. F., & Slutsker, I. (2000), Accuracy assessments of aerosol optical properties retrieved from AERONET sun and sky-radiance measurements. *Journal of Geophysical Research*, *105*, 9791–9806.

Friedl, M. A., McIver, D. K., Hodges, J. C. F., Zhang, X. Y., Muchoney, D., Strahler, A. H., Woodcock, C. E., Gopal, S., Schneider, A., Cooper, A., Baccini, A., Gao, F., & Schaaf, C. (2002), Global land cover mapping from MODIS: Algorithms and early results. *Remote Sensing of Environment*, 83, 287–302.

Grenfell, T. C., & Warren, S. G. (1994), Reflection of solar radiation by the Antarctic snow surface at ultraviolet, visible and near-infrared wavelengths. *Journal of Geophysical Research*, *99*, 18669–18684.

Grenfell, T. C., & Perovich, D. K. (2004), Seasonal and spatial evolution of albedo in a snow-ice-land-ocean environment. *Journal of Geophysical Research*, *109*, C01001, doi:10.1029/2003JC001866.

Greuell, W., & Oerlemans, J. (2005), Validation of AVHRR- and MODIS-derived albedos of snow and ice surfaces by means of helicopter measurements. *Journal of Glaciology*, *51*, 37–48.

Hall, D. K. and G.A. Riggs (in press), Assessment of errors in the MODIS suite of snow-covered products. Hydrological Processes.

Hall, D. K., Riggs, G. A., & Salomonson, V. V. (2006), MODIS Snow and Sea Ice Products in *Earth Science Satellite Remote Sensing - Volume I: Science and Instruments*, edited by J. J. Qu, W. Gao, M. Kafatos, R.E. Murphy & V.V. Salomonson, Springer, New York, pp. 154 -181.

Hall, D. K., Foster, J. L., Irons, J. R., & Dabney, P. W. (1993), Airborne bidirectional radiances of snow-covered surfaces in Montana, U.S.A. *Annals of Glaciology*, *17*, 35–40.

Holben, B. N., Eck, T. F., Slutsker, I., Tanré, D., Buis, J. P., Setzer, A., Vermote, E., Reagan, J. A., Kaufman, Y. J., Nakajima, T., Lavenu, F., Jankowiak, I., & Smirnov, A. (1998), AERONET—A federated instrument network and data archive for aerosol characterization. *Remote Sensing of Environment*, *66*, 1–16.

Jin, Y., Schaaf, C., Gao, F., Li, X., Strahler, A., Zeng, X., & Dickinson, R. (2002), How does snow impact the albedo of vegetated land surfaces as analyzed with MODIS data? *Geophysical Research Letters*, *29*, doi:10.1029/2001GL014132.

King, M. D., & Herring, D. D. (2000), Monitoring Earth's vital signs. *Scientific American*, *282*, 72–77.

King, M. D., Menzel, W. P., Kaufman, Y. J., Tanré, D., Gao, B. C., Platnick, S., Ackerman, S. A., Remer, L. A., Pincus, R., & Hubanks, P. A. (2003), Cloud and aerosol properties, precipitable water, and profiles of temperature and humidity from MODIS. *IEEE Transactions on Geoscience and Remote Sensing*, *41*, 442–458.

King, M. D., Platnick, S., Yang, P., Arnold, G. T., Gray, M. A., Riédi, J. C., Ackerman, S. A., & Liou, K. N. (2004), Remote sensing of liquid water and ice cloud optical thickness and effective radius in the arctic: Application of airborne multispectral MAS data. *Journal of Atmospheric and Oceanic Technology*, *21*, 857–875.

Klein, A. G., & Stroeve, J. (2002), Development and validation of a snow albedo algorithm for the MODIS instrument. *Annals of Glaciology*, *34*, 45–52.

Liang S., Fang, H., Chen, M., Shuey, C. J., Walthall, C., Daughtry, C., Morisette, J., Schaaf, C., & Strahler, A. (2002), Validating MODIS land surface reflectance and albedo products: Methods and preliminary results. *Remote Sensing of Environment*, *83*, 149–162.

Liang. S., Stroeve, J., & Box, J. E. (2005), Mapping daily snow/ice shortwave broadband albedo from Moderate Resolution Imaging Spectroradiometer (MODIS): The improved direct retrieval algorithm and validation with Greenland in situ measurement. *Journal of Geophysical Research*, *110*, D10109, doi:10.1029/2004JD005493.

McFadden, J. D., & Ragotzkie, R. A. (1967), Climatological significance of albedo in central Canada. *Journal of Geophysical Research*, *72*, 1135–1143.

Molotch, N. P., & Bales, R. C. (2006), Comparison of ground-based and airborne snow surface albedo parameterizations in an alpine watershed: Impact on snowpack mass balance. *Water Resources Research*, *42*, W05410, doi:10.1029/2005WR004522.

Molotch, N. P., Painter, T. H., Bales, R. C., & Dozier, J. (2004), Incorporating remotely sensed snow albedo into spatially distributed snowmelt modeling. *Geophysical Research Letters*, *31*, L03501, doi:10.1029/2003GL019063.

Moody, E. G., King, M. D., Platnick, S., Schaaf, C. B., & Gao, F. (2005), Spatially complete global spectral surface albedos: Value-added datasets derived from Terra MODIS land products. *IEEE Transactions on Geoscience and Remote Sensing*, *43*, 144–158.

Moody, E. G., King, M. D., Platnick, S., & Schaaf, C. B. (2007), Temporal and spatial trends in the MODIS-derived spatially complete global spectral surface albedo products. Submitted to *Journal of Climate.*

Nolin, A. W., & Dozier, J. (2000), A hyperspectral method for remotely sensing the grain size of snow. *Remote Sensing of Environment*, *74*, 207–216.

O'Brien, H. W., & Munis, R. H. (1975), *Red and Near-Infrared Spectral Reflectance of Snow,* Research Report 332, Cold Regions Research and Engineering Laboratory, Cold Spring Harbor, NY, 18 pp.

Platnick, S., King, M. D., Ackerman, S. A., Menzel, W. P., Baum, B. A., Riédi, J. C., & Frey, R. A. (2003), The MODIS cloud products: Algorithms and examples from Terra. *IEEE Transactions on Geoscience and Remote Sensing*, *41*, 459–473.

Pomeroy, J. W., & Dion, K. (1996), Winter radiation extinction and reflection in a boreal pine canopy: Measurements and modeling. *Hydrological Processes*, *10*, 1591-1608.

Robinson, D. A., & Kukla, G. (1985), Maximum surface albedo of seasonally snow-covered lands in the Northern Hemisphere. *Journal of Climate and Ap-*

plied Meteorology, 24, 402–411.

Roesch, A., Wild, M., Pinker, R., & Ohmura, A. (2002), Comparison of spectral surface albedos and their impact on the general circulation model simulated surface climate. *Journal of Geophysical Research*, *107*, 4221, doi:10.1029/2001JD000809.

Salomonson, V. V., & Marlatt, W. E. (1968), Anisotropic solar reflectance over white sand, snow and stratus clouds. *Journal of Applied Meteorology*, *7*, 475–483.

Stroeve, J., Box, J., Gao, F., Liang, S., Nolin, A., & Schaaf, C. (2005), Accuracy assessment of the MODIS 16-day albedo product for snow: Comparisons with Greenland in situ measurements. *Remote Sensing of Environment*, *94*, 46–60.

Schaaf, C. B., Gao, F., Strahler, A. H., Lucht, W., Li, X. W., Tsang, T., Strugnell, N. C., Zhang, X. Y., Jin, Y. F., Muller, J. P., Lewis, P., Barnsley, M., Hobson, P., Disney, M., Roberts, G., Dunderdale, M., Doll, C., d'Entremont, R. P., Hu, B. X., Liang, S. L., Privette, J. L., & Roy, D. (2002), First operational BRDF, albedo nadir reflectance products from MODIS. *Remote Sensing of Environment*, *83*, 135–148.

Verseghy, D. L. (1991), CLASS—A Canadian land surface scheme for GCMs. Part I: Soil model. *International Journal of Climatology*, *11*, 111–133.

Viterbo, P., & Betts, A. K. (1999), Impact on ECMWF forecasts of changes to the albedo of the boreal forests in the presence of snow. *Journal of Geophysical Research*, *104*, 27803–27810.

Warren, S. G. (1982), Optical properties of snow. *Reviews of Geophysics and Space Physics*, *20*, 67–89.

Warren, S. G., & Wiscombe, W. J. (1980), A model for the spectral albedo of snow. II: Snow containing atmospheric aerosols. *Journal of the Atmospheric Sciences,* *37*, 2734–2745.

Wiscombe, W. J., & Warren, S. G. (1980), A model for the spectral albedo of snow. I: Pure snow. *Journal of the Atmospheric Sciences*, *37*, 2712–2733.

Yang, Z. L., Dickinson, R. E., Hahmann, A. N., Niu, G. Y., Shaikh, M., Gao, X., Bales, R. C., Sorooshian, S., & Jin, J. M. (1999), Simulation of snow mass and extent in global climate models. *Hydrological Processes*, *13*(12-13), 2097–2113.

TABLE CAPTIONS

Table 1. Mean values of Northern Hemisphere five-year (2000-2004) spectral white-sky surface albedo data (in the presence of snow) aggregated by IGBP ecosystem classification.

Table 2. Standard deviation values of Northern Hemisphere five-year (2000-2004) spectral white-sky surface albedo data (in the presence of snow) aggregated by IGBP ecosystem classification.

Table 1. Mean values of Northern Hemisphere five-year (2000-2004) spectral white-sky surface albedo data (in the presence of snow) aggregated by IGBP ecosystem classification.

	White-sky snow albedo by wavelength (μm)									
Ecosystem	0.47	0.55	0.69	0.86	1.24	1.64	2.13	0.3-0.7	0.7-5.0	0.3-5.0
Evergreen Needle Forest	0.36	0.36	0.33	0.40	0.24	0.09	0.05	0.31	0.24	0.27
Evergreen Broad Forest	0.49	0.49	0.47	0.50	0.31	0.11	0.06	0.44	0.33	0.38
Deciduous Needle Forest	0.43	0.42	0.41	0.42	0.26	0.12	0.07	0.39	0.27	0.33
Deciduous Broad Forest	0.43	0.43	0.41	0.46	0.26	0.10	0.06	0.35	0.27	0.31
Mixed Forest	0.39	0.39	0.37	0.43	0.25	0.10	0.05	0.32	0.25	0.29
Closed Shrubs	0.48	0.48	0.46	0.47	0.29	0.11	0.06	0.42	0.30	0.36
Open Shrubs	0.73	0.72	0.70	0.67	0.37	0.12	0.06	0.68	0.44	0.56
Woody Savanna	0.47	0.46	0.44	0.47	0.28	0.11	0.06	0.44	0.30	0.37
Savanna	0.59	0.59	0.58	0.59	0.31	0.11	0.05	0.57	0.39	0.47
Grassland	0.72	0.72	0.71	0.70	0.39	0.12	0.06	0.70	0.48	0.59
Wetland	0.69	0.70	0.69	0.67	0.32	0.01	0.04	0.66	0.44	0.55
Cropland	0.76	0.76	0.76	0.74	0.40	0.11	0.05	0.69	0.47	0.58
Urban	0.54	0.54	0.53	0.55	0.30	0.11	0.06	0.50	0.34	0.42
Crop Mosaic	0.65	0.66	0.64	0.65	0.36	0.11	0.06	0.59	0.41	0.50
Permanent Snow	0.95	0.94	0.92	0.84	0.45	0.12	0.05	0.89	0.57	0.74
Barren/Desert	0.87	0.87	0.85	0.80	0.42	0.12	0.06	0.78	0.51	0.65

Table 2. Standard deviation values of Northern Hemisphere five-year (2000-2004) spectral white-sky surface albedo data (in the presence of snow) aggregated by IGBP ecosystem classification.

	Standard deviation of white-sky snow albedo by wavelength (μm)									
Ecosystem	0.47	0.55	0.69	0.86	1.24	1.64	2.13	0.3-0.7	0.7-5.0	0.3-5.0
Evergreen Needle Forest	0.11	0.12	0.12	0.11	0.06	0.02	0.01	0.14	0.08	0.10
Evergreen Broad Forest	0.14	0.15	0.16	0.14	0.08	0.03	0.02	0.17	0.11	0.14
Deciduous Needle Forest	0.08	0.08	0.08	0.08	0.06	0.02	0.01	0.10	0.07	0.08
Deciduous Broad Forest	0.11	0.11	0.12	0.10	0.07	0.02	0.02	0.12	0.08	0.09
Mixed Forest	0.14	0.14	0.15	0.12	0.07	0.02	0.01	0.14	0.09	0.11
Closed Shrubs	0.12	0.12	0.13	0.12	0.07	0.03	0.02	0.15	0.10	0.13
Open Shrubs	0.15	0.16	0.16	0.14	0.09	0.03	0.02	0.17	0.13	0.15
Woody Savanna	0.12	0.12	0.13	0.11	0.07	0.03	0.02	0.14	0.10	0.11
Savanna	0.12	0.12	0.12	0.11	0.09	0.03	0.02	0.14	0.10	0.12
Grassland	0.15	0.16	0.16	0.15	0.09	0.03	0.02	0.16	0.12	0.14
Wetland	0.12	0.12	0.12	0.11	0.11	0.04	0.02	0.14	0.11	0.12
Cropland	0.12	0.11	0.12	0.10	0.08	0.03	0.02	0.15	0.11	0.13
Urban	0.13	0.13	0.14	0.12	0.09	0.03	0.02	0.15	0.10	0.12
Crop Mosaic	0.17	0.17	0.17	0.14	0.09	0.03	0.01	0.18	0.12	0.15
Permanent Snow	0.07	0.06	0.07	0.09	0.10	0.04	0.02	0.11	0.11	0.11
Barren/Desert	0.10	0.10	0.11	0.11	0.09	0.03	0.02	0.16	0.13	0.14

FIGURE LEGENDS

Fig. 1. Mean values derived from five years of Northern Hemisphere white-sky spectral albedo data (in the presence of snow) as a function of IGBP ecosystem classification. The statistics are derived from 2000-2004 MOD43B3 collection 4, MOD12Q1, and NISE data. Sea ice is excluded from this analysis.

Fig. 2. November through April monthly mean values derived from five years of Northern Hemisphere white-sky spectral albedo data (in the presence of snow) as a function of eight (a-h) IGBP ecosystem classifications. For comparison, similarly derived, but snow-free five-year means of mature and dormant 16-day periods are presented. The statistics are derived from 2000-2004 MOD43B3 collection 4, MOD12Q1, and NISE data.

Fig. 3. November through April monthly mean values derived from five years of Northern Hemisphere white-sky spectral albedo data (in the presence of snow) as a function of eight (a-h) IGBP ecosystem classifications. For comparison, similarly derived, but snow-free five-year means of mature and dormant 16-day periods are presented. The statistics are derived from 2000-2004 MOD43B3 collection 4, MOD12Q1, and NISE data.

Fig. 4. Coefficient of variability values derived from five years of Northern Hemisphere white-sky spectral albedo data (in the presence of snow) as a function of IGBP ecosystem classification. The statistics are derived from 2000-2004 MOD43B3 collection 4, MOD12Q1, and NISE data. Sea ice is excluded from this analysis.

Fig. 5. 0.86 μm white-sky snow-free spatially complete albedo data from January 1-16, 2002, without (top) and with (bottom) overlaid snow albedo values. Pixels flagged as snow by the NISE snow extent product have

their snow-free values replaced with ecosystem-dependant snow-covered albedo values. The snow-covered albedo values are provided from the lookup table, Table 1.

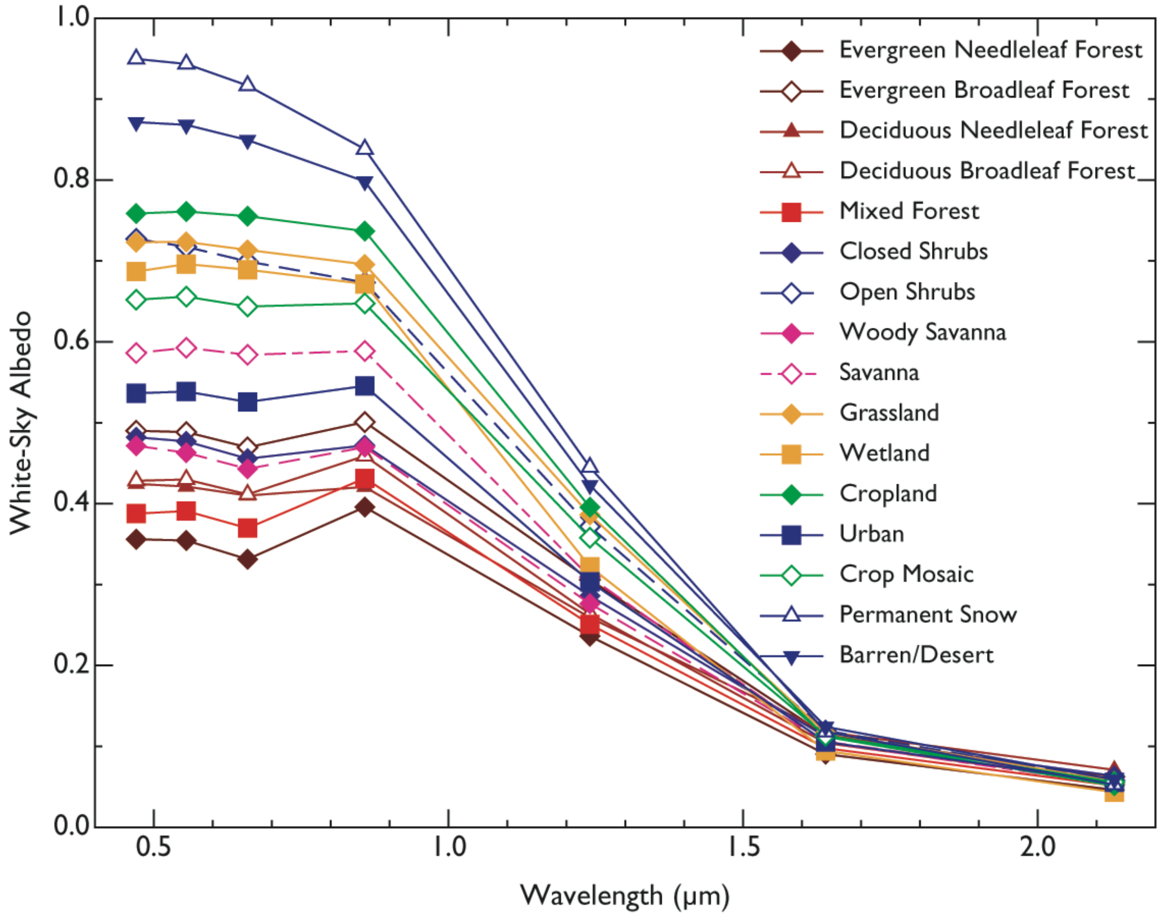

Fig. 1. Mean values derived from five years of Northern Hemisphere white-sky spectral albedo data (in the presence of snow) as a function of IGBP ecosystem classification. The statistics are derived from 2000-2004 MOD43B3 collection 4, MOD12Q1, and NISE data. Sea ice is excluded from this analysis.

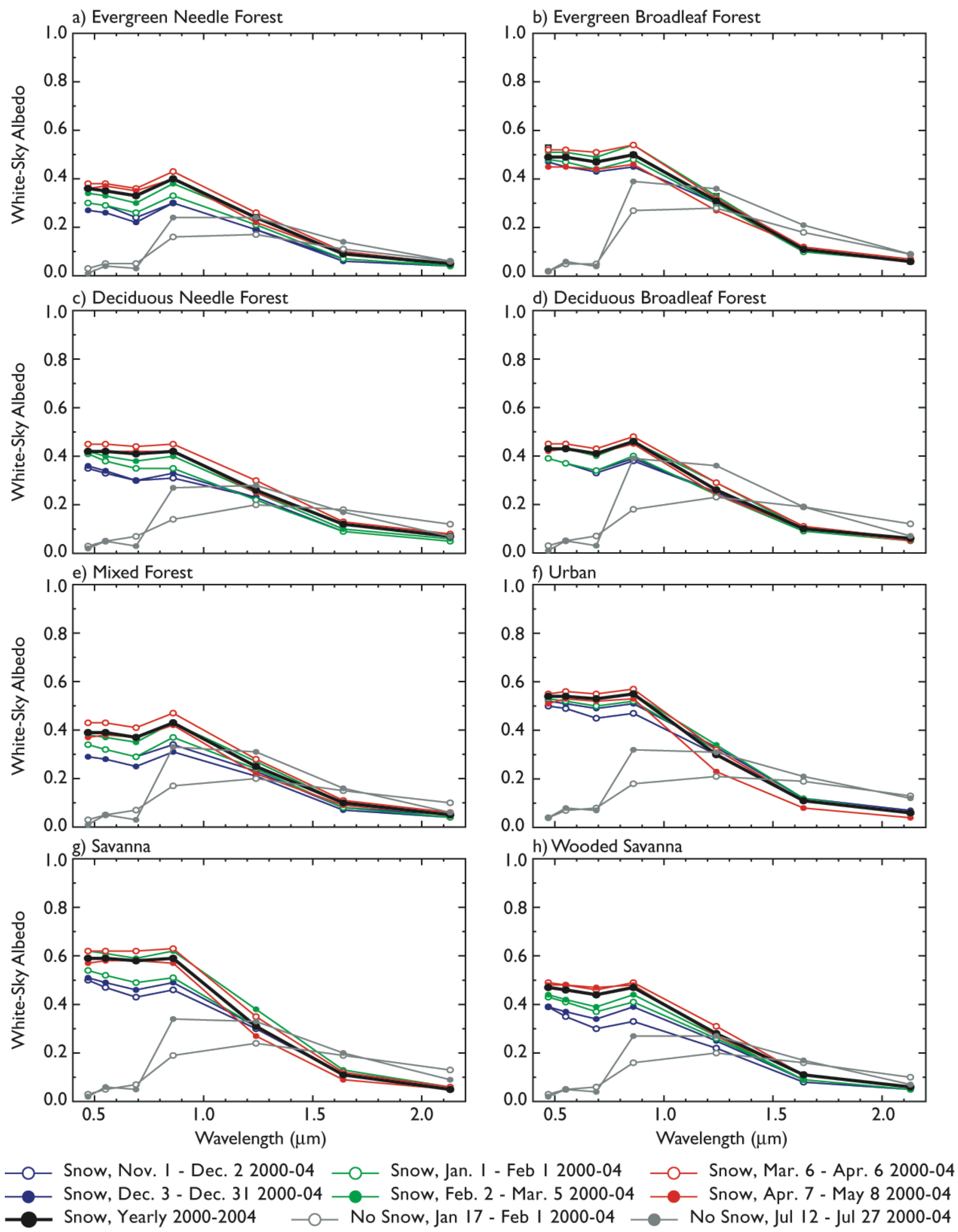

Fig. 2. November through April monthly mean values derived from five years of Northern Hemisphere white-sky spectral albedo data (in the presence of snow) as a function of eight (a-h) IGBP ecosystem classifications. For comparison, similarly derived, but snow-free five-year means of mature and dormant 16-day periods are presented. The statistics are derived from 2000-2004 MOD43B3 collection 4, MOD12Q1, and NISE data.

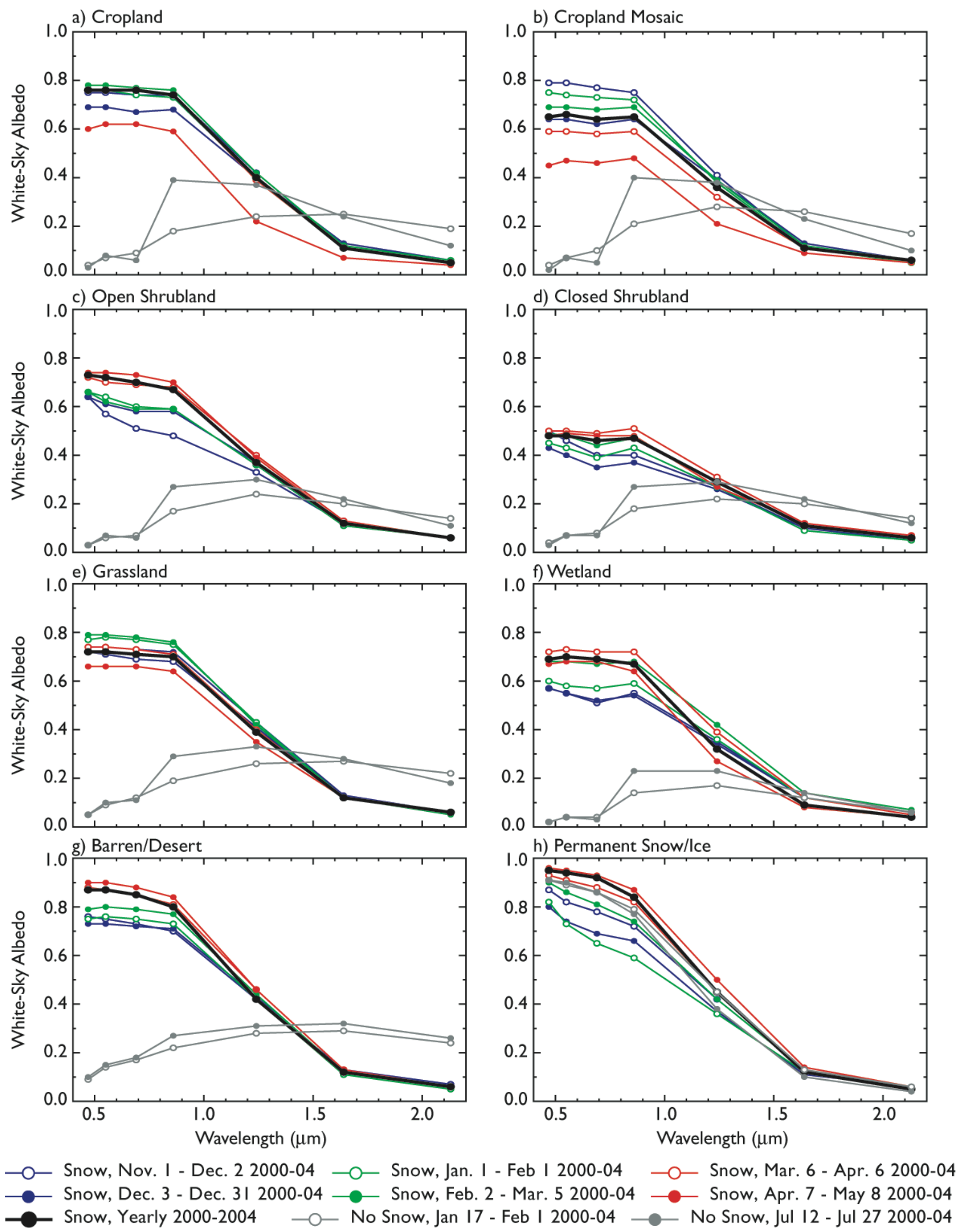

Fig. 3. November through April monthly mean values derived from five years of Northern Hemisphere white-sky spectral albedo data (in the presence of snow) as a function of eight (a-h) IGBP ecosystem classifications. For comparison, similarly derived, but snow-free five-year means of mature and dormant 16-day periods are presented. The statistics are derived from 2000-2004 MOD43B3 collection 4, MOD12Q1, and NISE data.

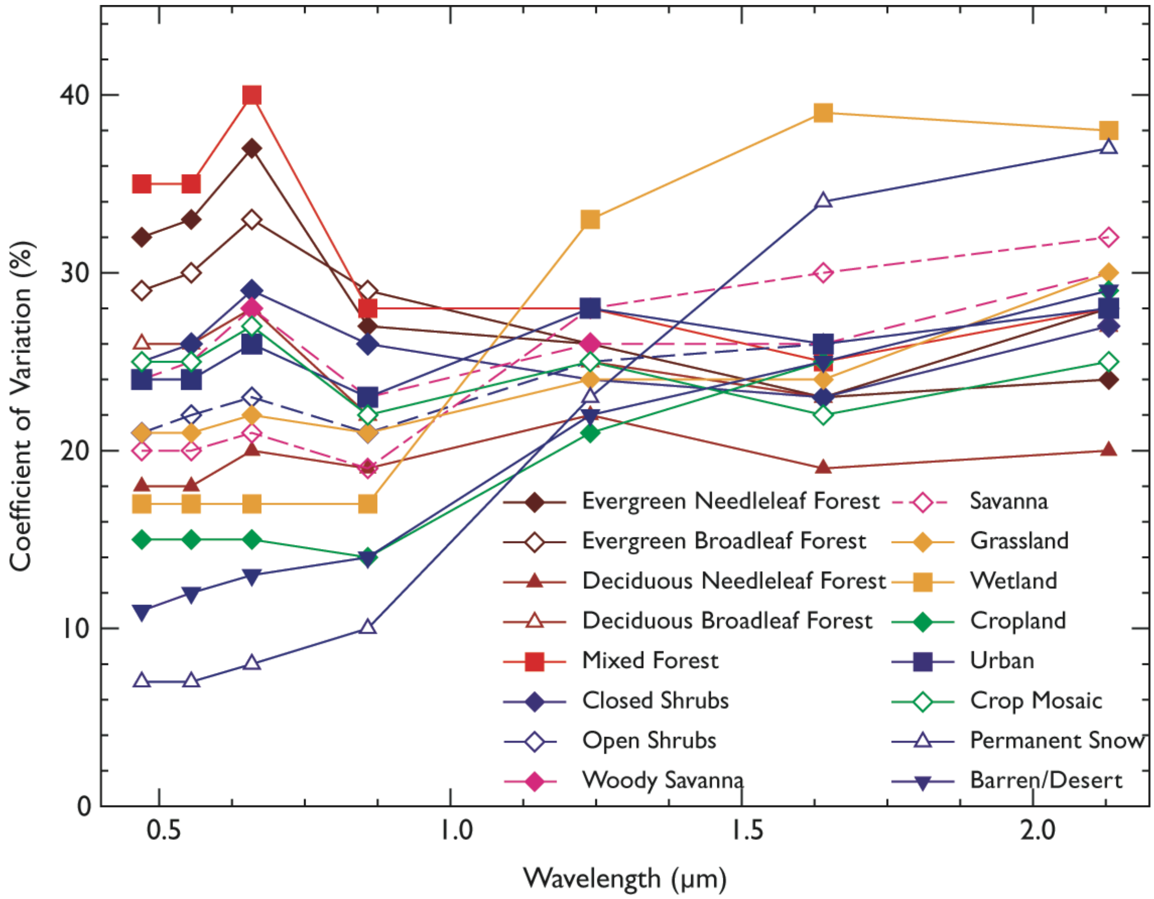

Fig. 4. Coefficient of variability values derived from five years of Northern Hemisphere white-sky spectral albedo data (in the presence of snow) as a function of IGBP ecosystem classification. The statistics are derived from 2000-2004 MOD43B3 collection 4, MOD12Q1, and NISE data. Sea ice is excluded from this analysis.

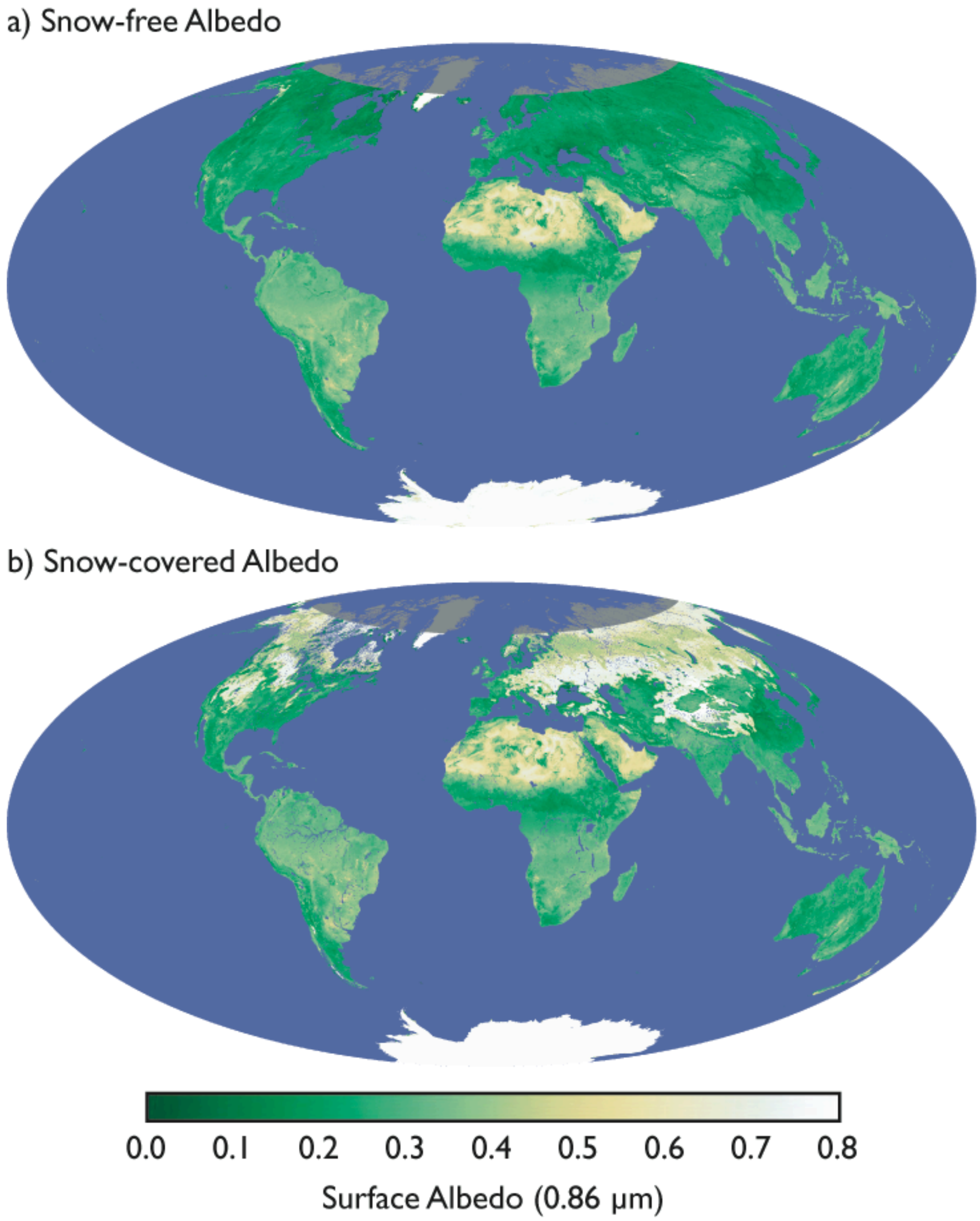

Fig. 5. 0.86 μm white-sky snow-free spatially complete albedo data from January 1-16, 2002, without (top) and with (bottom) overlaid snow albedo values. Pixels flagged as snow by the NISE snow extent product have their snow-free values replaced with ecosystem-dependant snow-covered albedo values. The snow-covered albedo values are provided from the lookup table, Table 1.